Research Article | Vol. 7, No. 7 | 1 Jul 2017 | OPTICAL MATERIALS EXPRESS 2293
Optical Materials EXPRESS

Refractive index measurements of photoresists for three-dimensional direct laser writing

TIMO GISSIBL,[1] SEBASTIAN WAGNER,[1] JACHYM SYKORA,[2] MICHAEL SCHMID,[1] AND HARALD GIESSEN[1,*]

[1]*4th Physics Institute and Research Center SCoPE, University of Stuttgart, Pfaffenwaldring 57, 70569 Stuttgart, Germany*
[2]*Max Planck Institute for Solid State Research, D-70569 Stuttgart, Germany*
[*]*giessen@physik.uni-stuttgart.de*

Abstract: Femtosecond 3D printing is an important technology for manufacturing of nano- and microscopic devices and elements. Crucial for the design of such structures is the detailed knowledge of the refractive index in the visible and near-infrared spectral range and its dispersion. Here, we characterize 5 photoresists that are used with femtosecond 3D direct laser writers, namely IP-S, IP-Dip, IP-L, IP-G, and OrmoComp with a modified and automized Pulfrich refractometer setup, utilizing critical angles of total internal reflection. We achieve an accuracy of $5 \cdot 10^{-4}$ and reference our values to a BK-7 glass plate. We also give Abbe numbers and Schott Catalog numbers of the different resists. Their refractive indices are in the 1.49-1.57 range, while their Abbe numbers are in the range between 35 and 51.

OCIS codes: (160.0160) Materials; (160.4760) Optical properties; (160.5335) Photosensitive materials, (260.2030) Dispersion.

References and links

1. M. F. Schumann, S. Wiesendanger, J. C. Goldschmidt, B. Bläsi, K. Bittkau, U. W. Paetzold, A. Sprafke, R. B. Wehrspohn, C. Rockstuhl, and M. Wegener, "Cloaked contact grids on solar cells by coordinate transformations: designs and prototypes," Optica **2**(10), 850–853 (2015).
2. M. Wegener, "Scharfe Linsen frisch gedruckt," Phys. J. **15**, 24–25 (2016).
3. J. Fischer and M. Wegener, "Three-dimensional optical laser lithography beyond the diffraction limit," Laser Photonics Rev. **7**(1), 22–44 (2013).
4. Z. Tian, X. Cao, W. Yao, P. Li, Y. Yu, G. Li, Q. Chen, and H. Sun, "Hybrid Refractive–Diffractive Optical Vortex Microlens," IEEE Photonics Technol. Lett. **28**(21), 2299–2302 (2016).
5. J. Xu, W. Yao, Z. Tian, L. Wang, K. Guan, Y. Xu, Q. Chen, J. Duan, and H. Sun, "High Curvature Concave–Convex Microlens," IEEE Photonics Technol. Lett. **27**(23), 2465–2468 (2015).
6. Z. N. Tian, W. G. Yao, J. J. Xu, Y. H. Yu, Q. D. Chen, and H. B. Sun, "Focal varying microlens array," Opt. Lett. **40**(18), 4222–4225 (2015).
7. D. Wu, S. Wu, L. Niu, Q. Chen, R. Wang, J. Song, H. Fang, and H. Sun, "High numerical aperture microlens arrays of close packing," Appl. Phys. Lett. **97**(3), 031109 (2010).
8. M. S. Rill, C. Plet, M. Thiel, I. Staude, G. von Freymann, S. Linden, and M. Wegener, "Photonic metamaterials by direct laser writing and silver chemical vapour deposition," Nat. Mater. **7**(7), 543–546 (2008).
9. M. Thiel, A. Radke, B. Fries, D. Eicke, F. Niesler, C. Baretzky, T. Bückmann, and M. Wegener, "High-Speed 3D Direct Laser Writing of Micro-Optical Elements," in *CLEO: 2013*, OSA Technical Digest (online) (Optical Society of America, 2013), paper ATu2N.4.
10. S. Thiele, T. Gissibl, H. Giessen, and A. M. Herkommer, "Ultra-compact on-chip LED collimation optics by 3D femtosecond direct laser writing," Opt. Lett. **41**(13), 3029–3032 (2016).
11. T. Gissibl, M. Schmid, and H. Giessen, "Spatial beam intensity shaping using phase masks on single-mode optical fibers fabricated by femtosecond direct laser writing," Optica **3**(4), 448–451 (2016).
12. T. Gissibl, S. Thiele, A. Herkommer, and H. Giessen, "Two-photon direct laser writing of ultracompact multi-lens objectives," Nat. Photonics **10**(8), 554–560 (2016).
13. T. Gissibl, S. Thiele, A. Herkommer, and H. Giessen, "Sub-micrometre accurate free-form optics by three-dimensional printing on single-mode fibres," Nat. Commun. **7**, 11763 (2016).
14. S. Thiele, K. Arzenbacher, T. Gissibl, H. Giessen, and A. M. Herkommer, "3D-printed eagle eye: Compound microlens system for foveated imaging," Sci. Adv. **3**(2), e1602655 (2017).
15. D. B. Fullager, G. D. Boreman, and T. Hofmann, "Infrared dielectric response of nanoscribe IP-dip and IP-L monomers after polymerization from 250 cm^{-1} to 6000 cm^{-1}," Opt. Mater. Express **7**(3), 888–894 (2017).

#291435 https://doi.org/10.1364/OME.7.002293
Journal © 2017 Received 27 Mar 2017; revised 20 May 2017; accepted 23 May 2017; published 9 Jun 2017

Optical Materials EXPRESS

16. J. Guild, "Notes on the Pulfrich Refractometer," Proc. Phys. Soc. Lond. **30**(1), 157–189 (1917).
17. B. Schaefer, *Lehrbuch der Experimentalphysik Band 3 Optik*, 10th ed., de Gruyter, NY and Berlin (2004), p. 70.
18. A. G. Schott, "Optisches Glas Datenblätter", (2016), http://www.schott.com/d/advanced_optics/47d79895-2965-472d-83ed-af9e48ac72c0/1.1/schott-optisches-glas-datenblatt-sammlung-german-17012017.pdf
19. F. A. Jenkins and H. E. White, *Fundamentals of Optics*, 4th ed., McGraw-Hill, Inc. (1981), p. 479.

1. Introduction

The dispersion of optical materials is an essential information for the design of high quality optical systems. In order to improve the optical performance, such as imaging quality and resolution, dispersion effects have to be taken into account.

Particularly, the fabrication of micro- and nanooptical elements by 3D direct laser writing using femtosecond pulses [1–11] and the possibility to fabricate multi-element microobjectives [12–14] requires precise refractive index data. The chance to design and realize achromatic multiple element lenses requires also accurate dispersion data. Additionally, absorption data, particularly in the infrared region, has become available recently through a pioneering paper by Hofman et al. [15].

As dispersion data of photosensitive materials are missing to our knowledge we measure the refractive indices at different wavelengths and determine the functional dependency. For this purpose, we measure the critical angle of total internal reflection of the used photoresists. In particular, Nanoscribe IP-Dip, micro resist OrmoComp, Nanoscribe IP-G, Nanoscribe IP-L, and Nanoscribe IP-S are analyzed.

The critical angle of total internal reflection is measured in the modified Pulfrich refractometer [16, 17] setup, which is a variant of critical angle refractometers, as depicted in Fig. 1(a). Linearly polarized light of a laser diode is directed through an astronomical telescope onto the base of a prism. The angle of the incident beam onto the base of the prism is controlled by a rotation mount. The astronomical telescope ensures that there is nearly no beam walk on the back of the prism, see Fig. 1(b). The reflection is guided through another astronomical telescope on a photodiode.

2. Method

Using trigonometric functions and Snell's law, the angle γ (see Fig. 1(b) for the definition) can be calculated from the rotation angle α of the rotation mount by

$$\begin{aligned}\gamma(\alpha) &= \arcsin\left[\frac{n}{n_2}\sin\left(\arctan\left(\frac{f_1}{f_2}\tan(2\alpha)\right)\right)\right] \\ &\approx \frac{n}{n_2}\frac{f_1}{f_2}2\alpha \text{ for small rotation angles } \alpha,\end{aligned} \tag{1}$$

where n is the refractive index of the surrounding medium (air) and n_2 is the refractive index of the prism material. The astronomical telescope consists of two lenses with focal lengths of f_1 = 10 cm and f_2 = 6 cm. The distance between the two lenses is equal to the sum of the two focal lengths ($f_1 + f_2$).

As a 60° SF-11 prism is used, the incident angle on the back of the prism can be calculated as

$$\theta(\alpha) = 60° + \gamma(\alpha). \tag{2}$$

The critical angle θ_c is given by

$$\theta_c = \arcsin\left(\frac{n_2}{n_1}\right), \tag{3}$$

Optical Materials EXPRESS

where n_1 and n_2 are the refractive indices of the two materials. For total internal reflection it is $n_1 > n_2$. Light which hits the interface under an angle θ larger than the critical angle θ_c is completely internally reflected.

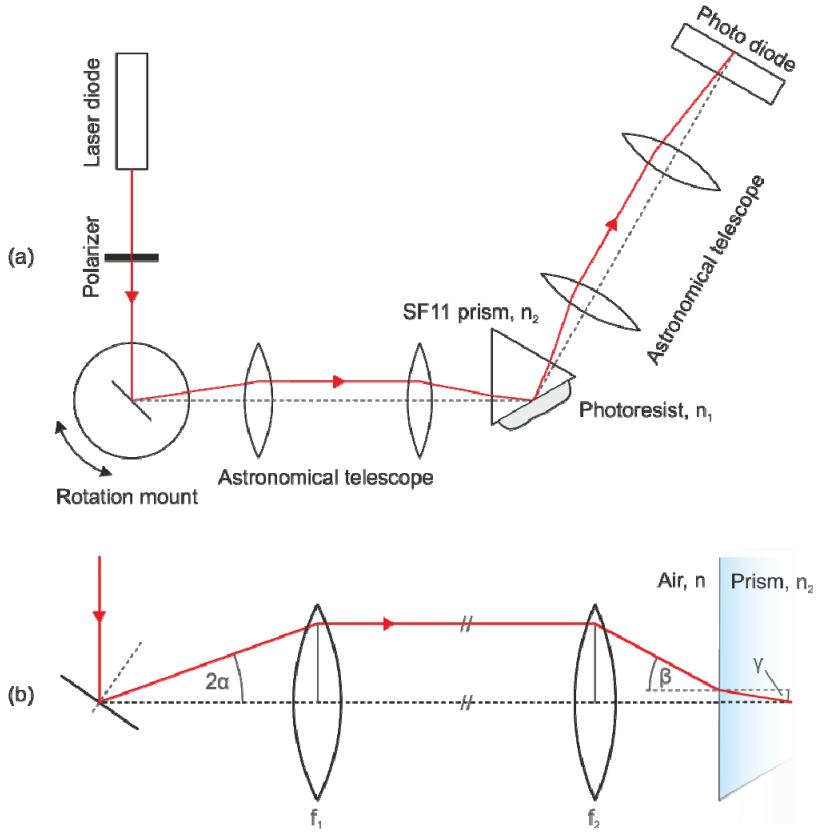

Fig. 1. Setup for measuring the critical angle of the total internal reflection, similar to a Pulfrich refractometer. (a) The refractive index values are obtained by measuring the critical angle of different photoresists at different wavelengths. The refractive index of the prism is n_2 and of the photoresist of interest is n_1. (b) Dependency of the angles in the setup for the refractive index measurement. The refractive indices of air (n) and prims material (n_2) are indicated.

The highly refractive SF 11 prism is required in order to obtain total internal reflection. By changing the angle θ of the incident beam the critical angle can be accurately determined. We measure the amount of reflected light using a photodiode. We use 5 different laser diodes with several mW output power at wavelengths of 450 nm, 532 nm, 650 nm, 780 nm, and 850 nm. The critical angle is then determined from the angular reflection curves for different photoresists at different incident laser wavelengths in s-polarization in order to calculate Cauchy's dispersion curves.

For each wavelength we determine the point of the critical angle of the prism/photoresist interface as well as for a prism/reference BK7 glass transition in order to calibrate the scale of the incident angle. For this purpose, the lower part of the prism is coated with an approximately 1 mm thick layer of the photoresist under investigation and subsequently, exposed by UV light for about 5 min (DymaxBlueWave 50 at a distance of 3 cm, delivering 365 nm with an intensity of 3000 mW/cm^2), on the upper part we optically bond a BK7 glass plate by pressure.

Optical Materials EXPRESS

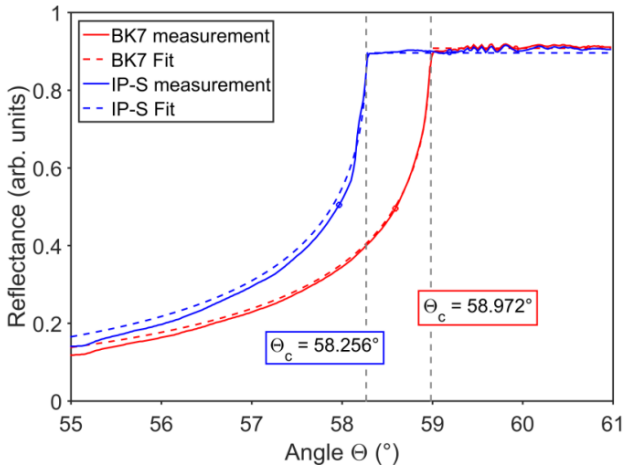

Fig. 2. Measurement of the critical angle of the total internal reflection of s-polarized light for OrmoComp and BK7 glass at a wavelength of 850 nm.

3. Experimental details

Figure 2 shows the angle dependent reflection measurement for IP-S and BK7 glass at a wavelength of 850 nm. We fit the functional relation of reflectance obtained by Fresnel's equation

$$R_s = \left| \frac{n_1 \cos\theta_1 - \sqrt{n_2^2 - n_1^2 \sin^2\theta_1}}{n_1 \cos\theta_1 + \sqrt{n_2^2 - n_1^2 \sin^2\theta_1}} \right|^2 \qquad (4)$$

for s-polarized light to the measurement data in order to determine the critical angle. The value of the critical angle of BK7 (whose refractive index is tabulated with great accuracy [18]) is used in order to calibrate the angle scale. The red curves represent the measurement of the BK7 glass, where the critical angle of θ_c is calculated by the literature values of 1.7619 and 1.5098 at a wavelength of 850 nm for SF11 and BK7, respectively [18]. The axis is accordingly adjusted with respect to the calculated value. Therefore, the critical angle of the photoresist can be accurately determined. The reflection curves are in good agreement with the theoretically expected reflectance behavior (Fresnel's equations) of the transition from a high to a low refractive index material.

Table 1. Refractive index measurement of the photoresists Nanoscribe IP-Dip, micro resist OrmoComp, Nanoscribe IP-G, Nanoscribe IP-L, and Nanoscribe IP-S. The refractive index values are obtained by measuring the critical angle of the total internal reflection for the used photoresists at different wavelengths. $n_{588\ nm}$ is interpolated from the Cauchy fit, however we list it here as it corresponds to the important value of n_d (at 587.6 nm).

Refractive indices	IP-S	IP-L	IP-G	OrmoComp	IP-Dip
$n_{450\ nm}$	1.5189	1.5272	1.5269	1.5315	1.5660
$n_{532\ nm}$	1.5103	1.5178	1.5187	1.5241	1.5534
$n_{588\ nm}$	1.5067	1.5140	1.5150	1.5207	1.5485
$n_{650\ nm}$	1.5039	1.5111	1.5120	1.5179	1.5446
$n_{780\ nm}$	1.4999	1.5074	1.5085	1.5140	1.5390
$n_{850\ nm}$	1.4985	1.5062	1.5072	1.5125	1.5367

Optical Materials EXPRESS

4. Results

Subsequently, we deposited different photoresists onto the SF11 glass prism, where on one part of the prism base surface the BK7 glass was optically fused by pressure and with the aid of carbon tetrachloride liquid, and on the other half of the prism base surface the resist was deposited. This way, we only needed to shift the prism vertically to carry out the two subsequent measurements. Table 1 shows the measured refractive indices of the photoresists IP-S (Nanoscribe), IP-L (Nanoscribe), IP-G (Nanoscribe), OrmoComp (micro resist technology), and IP-Dip (Nanoscribe). We compare the measured refractive index of OrmoComp with the values given in the datasheet of micro resist technology (n = 1.518 at 635 nm and n = 1.513 at 800 nm) and obtain excellent agreement.

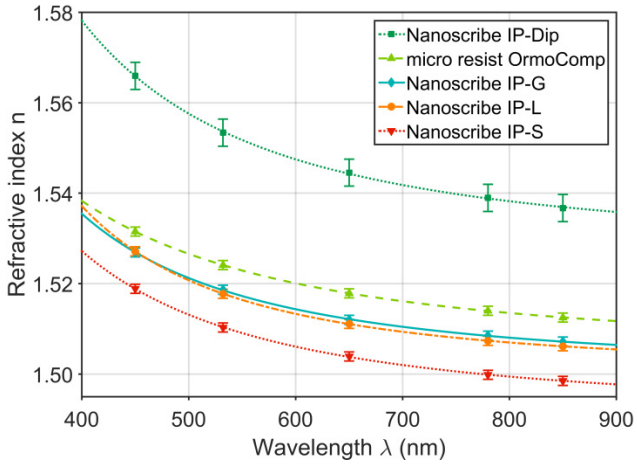

Fig. 3. Dispersion measurement of the photoresists. The refractive index characteristics is fitted by using Cauchy's equations. The error bars of IP-dip are slightly larger because of deviations from linearity of the trigonometric functions at larger angles.

In Fig. 3 the measurement results are displayed. We achieve an accuracy of $5 \cdot 10^{-4}$, only the error of IP-dip is larger ($3 \cdot 10^{-3}$) because of deviations from linearity of the trigonometric functions at larger angles. In addition, the refractive index characteristics is fitted by using Cauchy's equation [19] in the figure. The relationship between refractive index and wavelength is

$$n(\lambda) = A + \frac{B}{\lambda^2} + \frac{C}{\lambda^4}. \tag{5}$$

The fit parameters A, B, and C are summarized in Table 2. Cauchy's equation describes the measured values of the refractive indices quite well.

Table 2. Cauchy parameters of the photoresists Nanoscribe IP-Dip, micro resist OrmoComp, Nanoscribe IP-G, Nanoscribe IP-L, and Nanoscribe IP-S. The values are obtained by fitting Cauchy's equation to the refractive index measurements.

Cauchy parameters	A	B (μm^2)	C (μm^4)
Nanoscribe IP-S	1.4915	$4.8486 \cdot 10^{-3}$	$1.3694 \cdot 10^{-4}$
Nanoscribe IP-L	1.5003	$3.6771 \cdot 10^{-3}$	$3.5288 \cdot 10^{-4}$
Nanoscribe IP-G	1.5008	$4.3331 \cdot 10^{-3}$	$1.9364 \cdot 10^{-4}$
micro resist OrmoComp	1.5049	$5.5461 \cdot 10^{-3}$	$-3.3369 \cdot 10^{-5}$
Nanoscribe IP-Dip	1.5273	$6.5456 \cdot 10^{-3}$	$2.5345 \cdot 10^{-4}$

We use Cauchy's equation to calculate the Abbe number, which is a characteristic number for the dispersion of materials in optics. The Abbe number is defined as

Optical Materials EXPRESS

$$v_d = \frac{n_d - 1}{n_F - n_C}, \tag{6}$$

where n_d, n_F, and n_C are the refractive indices of the material at Fraunhofer lines d, F, and C. The Fraunhofer lines are associated with the absorption lines in the spectrum of the sun. d corresponds to a wavelength of 587.6 nm, F corresponds to a wavelength of 486.1 nm, and C corresponds to a wavelength of 656.3 nm.

The Abbe number of Nanoscribe IP-S is $\nu_d = 46.2$ and thus behaves similar to very light flint glasses. $\nu_d = 51.2$ is the Abbe number of micro resist OrmoComp, which is in the region of crown/flint glasses. Glasses which corresponds to the dispersion of IP-S and OrmoComp are for example LLF1 and N-KF9.

As the refractive indices of Nanoscribe IP-Dip are above the ones of IP-S and OrmoComp the Abbe number of IP-Dip is $\nu_d = 35.0$. Corresponding glasses are flint glasses. The Abbe numbers are summarized in Table 3:

Table 3. Abbe number ν_d and Schott catalog number of the photoresists Nanoscribe IP-Dip, micro resist OrmoComp, Nanoscribe IP-G, Nanoscribe IP-L, and Nanoscribe IP-S. The values are obtained by calculating the Abbe number with the Cauchy parameters.

	Abbe number ν_d	Schott catalog number
Nanoscribe IP-S	46.16	507462
Nanoscribe IP-L	44.92	514449
Nanoscribe IP-G	48.12	515481
micro resist OrmoComp	51.16	521512
Nanoscribe IP-Dip	34.98	549350

5. Conclusion

We measured the refractive index dispersion in the visible spectral range of five different photoresists that are used for 3D femtosecond direct laser writing. We determined the Cauchy parameters and the Abbe numbers as well as the equivalent Schott catalog numbers. This work will pave the way towards realization of achromatic 3D printed optical elements, as well as open the door towards using micro optical elements with tailored dispersive properties. Furthermore, our method represents the first step towards realization of an entire Abbe diagram with novel 3D printable material with tailorable refractive indices and dispersion properties.

Additionally, it is our experience that the refractive index is strongly dependent on the exposure dose, this means exposure time and intensity. First measurements show changes in the range of $5 \cdot 10^{-3}$. Furthermore, there is a time-dependent behavior of the refractive index directly after the exposure process, which reaches a plateau after a few hours. The exposure mode (UV exposure process or direct laser writing) influences the refractive index of the exposed photoresist, as well. These issues should be considered in a future evaluation, too.

Funding

DFG (GI 269/11-1); BMBF (13N10146, PRINTOPTICS and PRINTFUNCTION); Baden-Württemberg Stiftung (Spitzenforschung II and OPTERIAL); and ERC (COMPLEXPLAS).

Acknowledgments

We would like to thank Prof. J.-C. Buhl from the Department of Mineralogy at the University of Hannover for lending us two historic Pulfrich refractometers. This publication was supported by the Open Access Publishing Fund of the University of Stuttgart.